frontiers | Frontiers in Physics

TYPE Original Research
PUBLISHED 09 July 2025
DOI 10.3389/fphy.2025.1604033

OPEN ACCESS

EDITED BY
Shahin Agaev,
Baku State University, Azerbaijan

REVIEWED BY
Atif Arif,
COMSATS University, Pakistan
Fabrizio Grosa,
European Organization for Nuclear Research (CERN), Switzerland

*CORRESPONDENCE
Ning Yu,
ning.yuchina@gmail.com

RECEIVED 01 April 2025
ACCEPTED 20 June 2025
PUBLISHED 09 July 2025

CITATION
Xu H, She Z, Yu N and Zhang Z (2025) Production of the *X*(3872) in Pb-Pb collisions at $\sqrt{s_{NN}} = 5.02$ TeV from PACIAE model. *Front. Phys.* 13:1604033. doi: 10.3389/fphy.2025.1604033

Production of the *X*(3872) in Pb-Pb collisions at $\sqrt{s_{NN}} = 5.02$ TeV from PACIAE model

Hongge Xu[1,2], Zhilei She[3], Ning Yu[1,2]* and Zuman Zhang[1,2]

[1]School of Physics and Mechanical Electrical & Engineering, Hubei University of Education, Wuhan, China, [2]Institute of Astronomy and High Energy Physics, Hubei University of Education, Wuhan, China, [3]Wuhan Textile University, Wuhan, China

We employed the dynamically constrained phase space coalescence model to study the *X*(3872), where the parton and hadron cascade model (PACIAE) was used to simulate Pb-Pb collisions at $\sqrt{s_{NN}} = 5.02$ TeV in centralities of $0-10\%$ and $30-50\%$. In this work, we examined the correlation between the yield of the *X*(3872) and the parameters Δm and R. Additionally, We predicted the yields of the *X*(3872) for its three plausible configurations, namely, the hadronic molecular state, tetraquark state and nuclear-like state, in Pb-Pb collisions at $\sqrt{s_{NN}} = 5.02$ TeV. We also analyzed the transverse momenta for three different structures of the *X*(3872). Sizable differences were observed in the transverse momentum distributions among the three different *X*(3872) structures.

KEYWORDS

heavy ion collision, exotic hadron, hadronic molecular state, tetraquark state, nuclear-like state

1 Introduction

Hadron spectroscopy is a field replete with frequent discoveries and surprises, and the theoretical complexities associated with understanding the strong interaction in the color confinement regime make the field even more fascinating. A very successful classification scheme for hadrons in terms of their valence quarks and antiquarks was independently proposed by Murray Gell-Mann [1] and George Zweig [2] in 1964. This classification, known as the quark model, essentially divides hadrons into two major families: mesons (quark-antiquark) and baryons (three-quarks). Theoretically, the basic theory of the strong interaction, quantum chromodynamics (QCD), allows for the existence of exotic hadrons beyond the conventional picture.

The first quarkonium-like state, the *X*(3872), was discovered by the Belle collaboration in the decay $B^{\pm} \rightarrow K^{\pm}X(3872) \rightarrow K^{\pm}(\pi^{+}\pi^{-}J/\psi)$ in 2003 [3]. It was subsequently confirmed by other experiments [4–6]. With the development of experimental techniques and the accumulation of data, a number of hadronic states beyond the conventional two-quark meson and three-quark baryon picture have been observed in the last 2 decades which are popular candidates for exotic hadrons [7]. By now, many approaches have been used to disentangle the nature of the numerous exotic hadrons discovered, but some difficulties remain [8, 9]. The study of exotic hadrons is also one of the most important topics in hadron physics.

TABLE 1 The comparisons of the yield of D^0, π, K, and p between PACIAE model and the experimental data [43, 44] in $|y| < 0.5$, $0 < p_T < 20$ GeV/c for π, K, and p, $1 < p_T < 50$ GeV/c for D^0 meson, respectively.

Particle	0 – 10%		30 – 50%	
	PACIAE	ALICE	PACIAE	ALICE
π	1501.74	1538.65 ± 185.4	368.87	380.34 ± 40.22
K	228.53	247.95 ± 21.88	58.89	60.68 ± 4.99
p	68.64	68.04 ± 6.81	16.7	18.49 ± 1.72
D^0	6.60	6.819 ± 1.43	1.02	1.275 ± 0.366

The production yields of exotic states in high-energy collisions, which are expected to be strongly influenced by their internal structure, have received increasing attention [10–18]. The internal structure of exotic hadrons is still under debate. They are assumed to be loosely bound hadronic molecule, a compact tetraquark, or just a kinematic effect such as the triangle singularity, etc [8, 9]. The internal structure and interactions of compact multiquark states and hadronic molecular states have been extensively studied. The former are bound by the strong interaction directly, while the latter are bound by residual strong interaction [8, 9, 19].

The abundant number of quarks and antiquarks for both light and heavy flavors suggests that heavy-ion collisions provide an ideal environment for exotic hadron production, compared to electron-positron and proton-proton (or antiproton) collisions. The first evidence for the $X(3872)$ production in relativistic heavy ion collisions was reported by the CMS Collaboration [16]. In this work, we think that the $X(3872)$ may be a tetraquark, nuclear-like, or molecular state, and study their production using the dynamically constrained phase-space coalescence model (DCPC). We employ the parton and hadron cascade (PACIAE) model to simulate Pb-Pb collisions at $\sqrt{s_{NN}} = 5.02$ TeV in centralities of 0 – 10% and 30 – 50%. Using the DCPC, we then predict the yield and transverse momentum of the $X(3872)$.

2 Model

The PACIAE model [20–22] is a parton and hadron cascade model based on PYTHIA [23]. It has been successfully used to describe particle multiplicity, transverse momentum, rapidity distributions, and other observables in high-energy collisions [17, 24–27]. The PACIAE Monte-Carlo (MC) simulation provides a complete description of one collision, which includes the partonic initialization stage, partonic rescattering stage, hadronization stage, and the hadronic rescattering stage. For nucleon-nucleon (NN) collisions, compared to PYTHIA, the partonic and hadronic rescattering are introduced before and after the hadronization, respectively. The initial-state free parton is produced by breaking the strings of quarks, antiquarks, and gluons formed in the Pb-Pb collision with the PACIAE model. The parton rescattering is further considered using the $2 \rightarrow 2$ leading-order (LO) perturbative QCD parton-parton cross sections [28]. The total and differential cross section in the evolution of the deconfined quark matter state are calculated using MC method. After the partonic freeze-out, the hadronization of the partonic matter is executed by the LUND string fragmentation [23] or the MC coalescence model [20]. Hadron rescattering is performed based on the two-body collision until the hadronic freeze-out.

The DCPC model was proposed to study production of the light nuclei in pp collisions [29]. In the DCPC model, based on the quantum statistical mechanics [30, 31], we can estimate the yield of a single particle in the six-dimension phase space by an integral

$$Y_1 = \int_{E_a \le H \le E_b} \frac{d\vec{q}d\vec{p}}{h^3}, \tag{1}$$

Here, E_a, E_b, and H denote the energy threshold and the energy function of the particle, respectively. The variables $\vec{q}$ and $\vec{p}$ correspond to the coordinates and momenta of the particle in the center-of-mass frame of the collision at the moment after hadronization. Furthermore, the yield of a cluster consisting of N particles is defined as following:

$$Y_N = \int \cdots \int_{E_a \le H \le E_b} \frac{d\vec{q}_1 d\vec{p}_1 \cdots d\vec{q}_N d\vec{p}_N}{(h)^{3N}}. \tag{2}$$

Therefore, the yield of an $X(3872)$ consisting of $D\bar{D}^*$ cluster in the DCPC model can be calculated by.

$$Y_{X(3872)} = \int \cdots \int \delta_{12} \frac{d\vec{q}_1 d\vec{p}_1 d\vec{q}_2 d\vec{p}_2}{h^6}, \tag{3}$$

$$\delta_{12} = \begin{cases} 1 \text{ if} 1 \equiv D, 2 \equiv \bar{D}^*; \\ m_{X(3872)} - \Delta m \le m_{inv} \le m_{X(3872)} + \Delta m; \\ q_{12} \le R; \\ 0 \text{ otherwise.} \end{cases} \tag{4}$$

where,

$$m_{inv} = \sqrt{(E_1 + E_2)^2 - (\vec{p}_1 + \vec{p}_2)^2}. \tag{5}$$

The q_{12} denote the relative distance between D and $\bar{D}^*$. The R represents the radius of the cluster (a free parameter). Obviously, the relative distance between D and $\bar{D}^*$ (q_{12}) in the compact picture is shorter than that in the nuclear or molecular picture. Consequently, the radius R of the compact state is also smaller. We assumed to that the $X(3872)$ might exist in three different state: tetraquark, nuclear-like, or molecular state, each with a distinct radius. In our simulation, we distinguish these three structures of the $X(3872)$ based on the value of R. According to the radius of deuteron and the result in Refs. [15, 19], the $X(3872)$ is assumed to be a tetraquark state when $R < 1.0$ fm; a nuclear-like state when $1.0 < R < 1.74$ fm; a molecular state, when $1.74 < R < 10.0$ fm. The $m_{X(3872)}$ denotes the rest mass of $X(3872)$, and Δm refers to its mass uncertainty. The E_1, E_2 denote the energies of the two particles (D and $\bar{D}^*$), while $\vec{p_1}, \vec{p_2}$ represent their respective momenta.

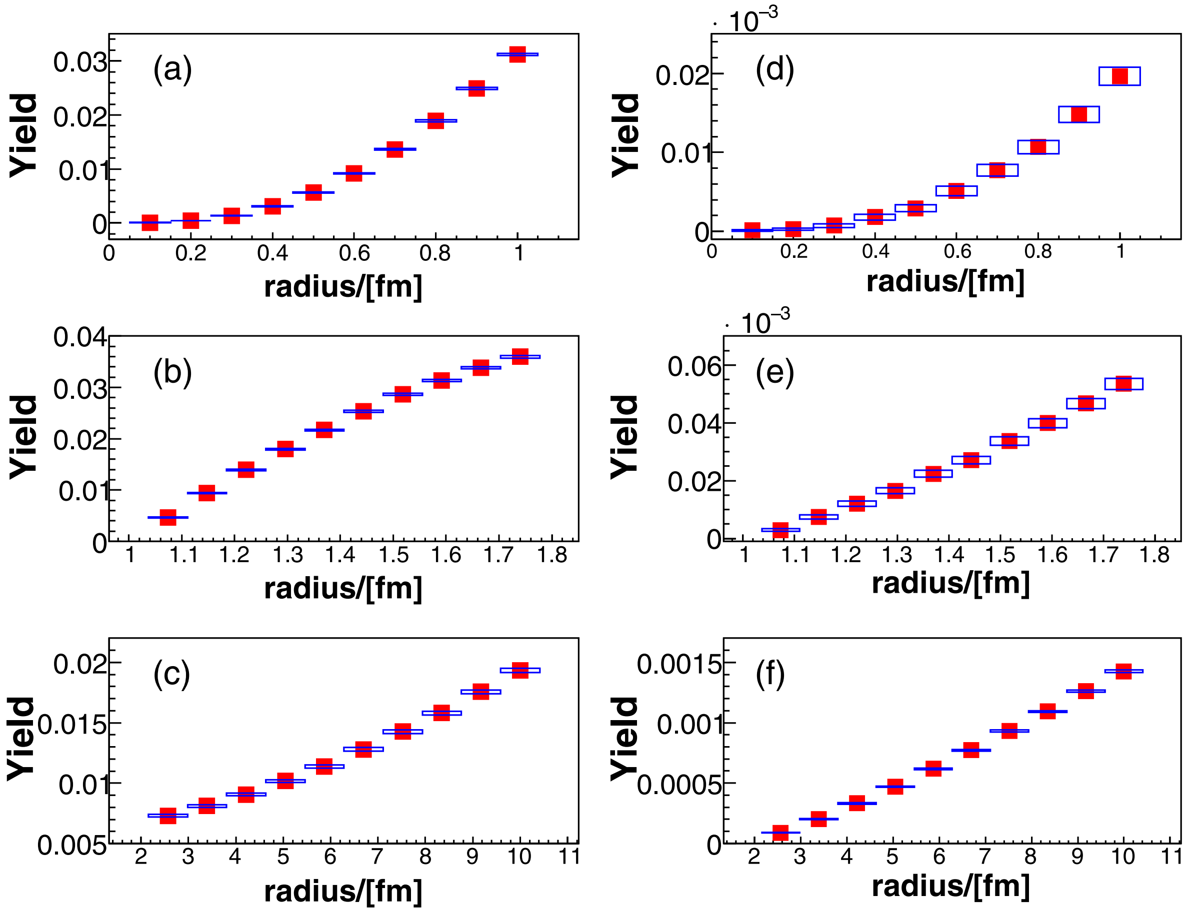

FIGURE 1
Radius distributions of $X(3872)$ Pb-Pb collisions at $\sqrt{s_{NN}} = 5.02$TeV. As a function of radius parameter R. The left and right hand plot is performed in centralities of 0 – 10% and 30 – 50%, respectively. The distribution in top, middle and bottom is for tetraquark, nuclear-like, molecular state. The blue empty markers indicates statistical uncertainties, red filled markers indicates data point by PACIAE + DCPC model.

The DCPC model has been successfully applied to different collision systems at RHIC and LHC, including $p-p$[13, 17, 32–35], Cu-Cu [36, 37], Au-Au [24, 38–40], and Pb-Pb [41, 42] collisions. Especially, it has been successfully used to calculate the yields of the exotic states following transport model simulations [13, 17, 34, 35].

3 Result

In this work, we produce the $X(3872)$ and investigate its nature in Pb-Pb collisions at $\sqrt{s_{NN}} = 5.02$ TeV within the 0 − −10% and 30 − −50% centrality ranges using PACIAE + DCPC. The production involves a two-step process: first, simulating Pb-Pb collisions at $\sqrt{s_{NN}} = 5.02$ TeV to generate the multi-particle final states; then, combining the final states D^0, $\bar{D}^0$, D^{0*} and $\bar{D}^{0*}$ to generate the tetraquark, nuclear-like and molecular states of the $X(3872)$ using DCPC model.

In the production of final states particles with PACIAE, the impact parameter b is set to $0 - 4.89$, and $8.47 - 10.93$, according to Ref. [45], to simulate Pb-Pb collisions in the centrality ranges of 0 − −10% and 30 − −50%, respectively. The other model parameters are fixed at their default values given in the PYTHIA model, expect for the K factor and the parameters parj (1), parj (2), and parj (3). Here, the K factor is introduced to include the higher order and the nonperturbative corrections, parj (1) represents the suppression of diquark–antidiquark pair production relative to the quark–antiquark pair production, parj (2) denotes the suppression of strange quark pair production relative to up (down) quark pair production, parj (3) indicates the extra suppression for strange diquark production compared to the normal suppression of a strange quark. These parameters are determined by fitting to the ALICE data [43, 44] for D^0, π, K, and p in Pb-Pb collisions at $\sqrt{s_{NN}} = 5.02$TeV. The comparison of the yields for each final states between the simulation from the PACIAE model with determined parameters and the experimental measurements by ALICE collaboration is shown in Table 1, which are consistent with each other within uncertainties.

In this work, the $X(3872)$ states are generated by combining the final state particles D^0 and $\bar{D}^{0*}$ (or $\bar{D}^0$ and D^{0*}) using the DCPC model, following the simulation of Pb-Pb collisions by the PACIAE model. First, we calculate the yield of the

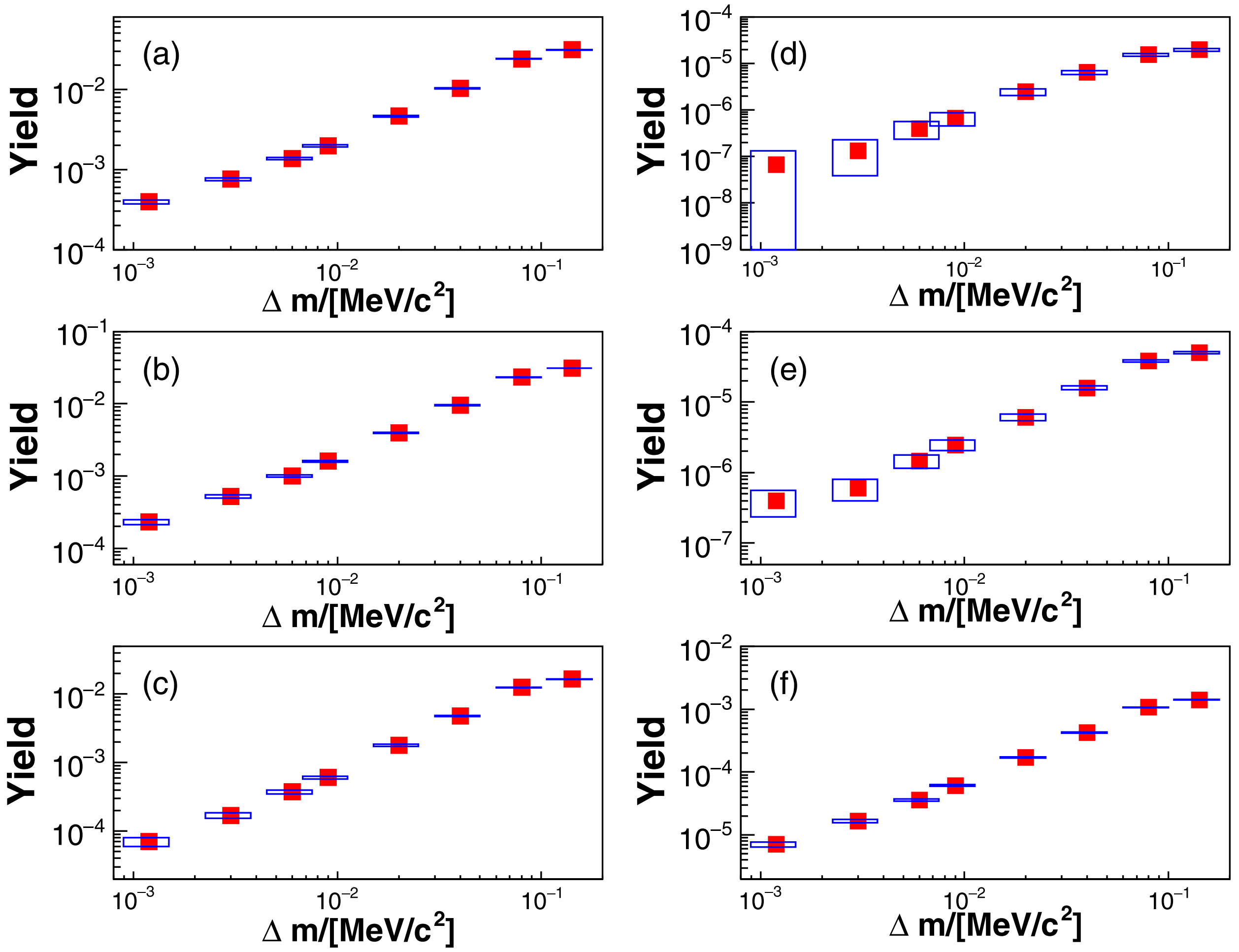

FIGURE 2
Mass distributions of the $X(3872)$ in Pb-Pb collisions at $\sqrt{s_{NN}} = 5.02$TeV as a function of mass uncertainty Δm. The left and right hand plots correspond to centralities of 0 – 10% and 30 – 50%, respectively. The distribution in top, middle and bottom is for tetraquark, nuclear-like, molecular state. The blue empty markers indicate statistical uncertainties, while red filled markers indicate data points obtained by PACIAE + DCPC model.

TABLE 2 The yield of $X(3872)$ with three states in 0%–10% and 30%–50% Pb-Pb collisions at $\sqrt{s_{NN}} = 5.02$TeV.

Centrality	Tetraquark	Nuclear-like	Molecular
0 – 10%	3.12×10^{-2}	3.11×10^{-2}	1.65×10^{-2}
30 – 50%	1.96×10^{-5}	5.02×10^{-5}	1.41×10^{-3}

$X(3872)$ in Pb-Pb collisions at $\sqrt{s_{NN}} = 5.02$TeV, with parameter R varying from 1.0 fm to 10.0 fm, at a given mass uncertainty $\Delta m = 142\text{MeV}/c^2$ (obtained from $2m_D < m_{inv} < 2m_{\bar{D}^*}$ [18]). Depending on the value of R, the exotic state $X(3872)$ can be classified into three structures: the tetraquark state for $R < 1.0$ fm, the nuclear-like state for $1.0 < R < 1.74$ fm, and the molecular state for $1.74 < R < 10$ fm. They are denoted as $X_T(3872)$, $X_N(3872)$ and $X_M(3872)$, respectively [15, 19]. Figure 1 present the distribution of the yield of these three different structures of the $X(3872)$ as a function of the parameter R. From Figure 1, we can conclude that the yield of each structure of the $X(3872)$ increase with parameter R at a given mass uncertainty $\Delta m = 142\text{MeV}/c^2$.

Then, we calculate the yields of three structures of the $X(3872)$ in Pb-Pb collisions as parameter Δm increases from 0.595 MeV (the half of the width of $X(3872)$) to 142 MeV. The distribution of the yield of the $X(3872)$ as a function of Δm is shown in Figure 2. From Figure 2, we observe that the yields of $X(3872)$ increase exponentially with increasing Δm.

As a reasonable prediction, we can predict the yields of the $X(3872)$ by assuming a mass uncertainty of $\Delta m = 142\text{MeV}/c^2$ (obtained from $2m_D < m_{inv} < 2m_{\bar{D}^*}$ [18]). The predicted yields of the $X(3872)$ in Pb-Pb collision at $\sqrt{s} = 5.02$TeV within 0 – 10% and 30 – 50% centrality ranges are shown in Table 2. From these results, We observe that the yield is larger in central collisions. When comparing the yield in central Pb-Pb collision with pp collisions, we find that the yield in pp collision is lower.

Moreover, we calculate the transverse momentum distribution of the tetraquark, nuclear-like and molecular states the $X(3872)$. Figure 3 shows the transverse momentum p_T distributions of these three different structures of the $X(3872)$ in Pb-Pb collision at

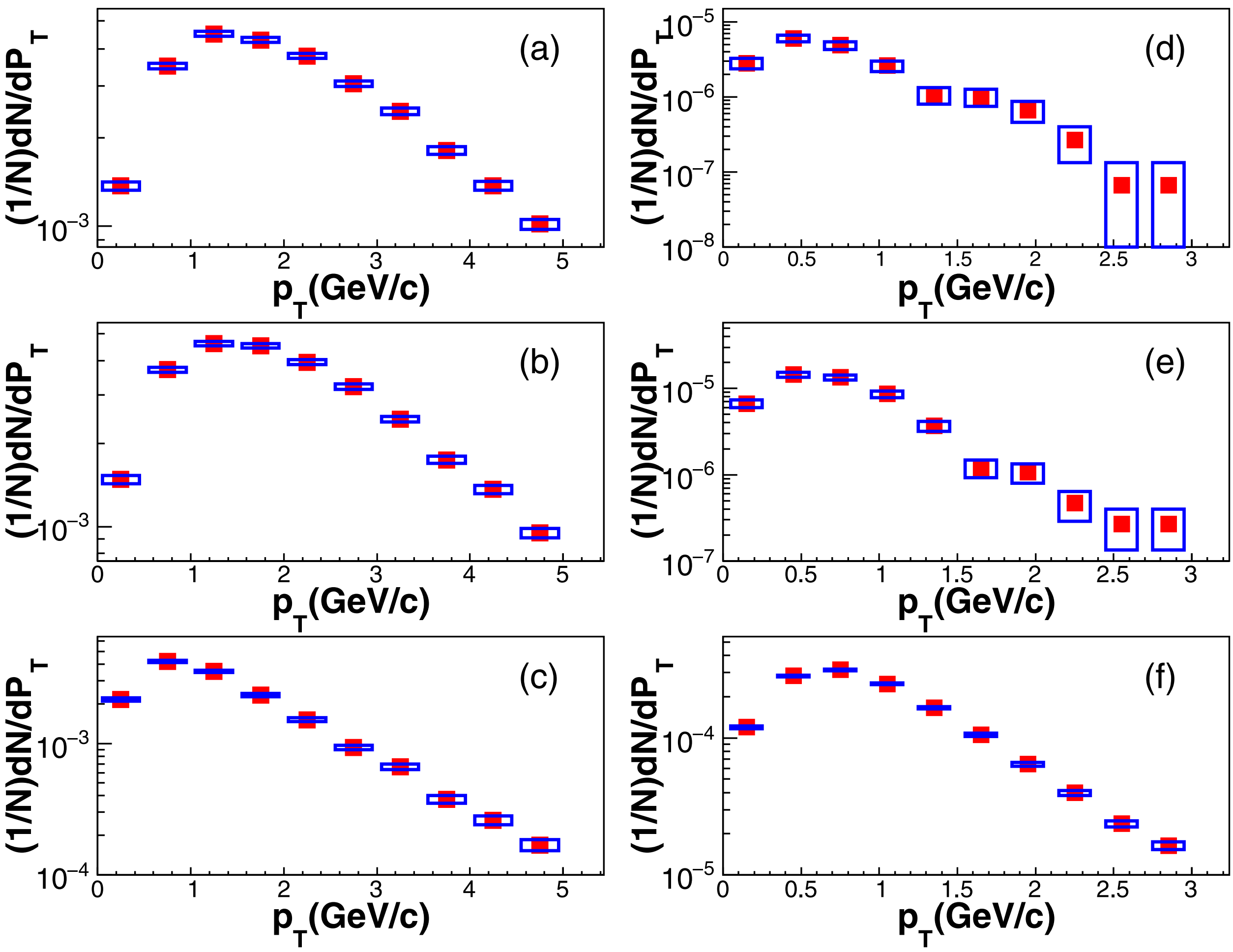

FIGURE 3
The transverse momentum distributions of the $X(3872)$ as a tetraquark state, nuclear-like state and molecular state. The left and right hand plot correspond to centralities of 0 – 10% and 30 – 50%, respectively. The distribution in top, middle and bottom represent the tetraquark, nuclear-like, molecular state, respectively. The blue empty markers indicate statistical uncertainties, while the red filled markers indicate data point by PACIAE + DCPC model.

$\sqrt{s_{NN}} = 5.02$TeV, for centralities of 0 – 10% and 30 – 50%. Obviously, the p_T distributions of the $X(3872)$ for the three different structures are similar to each other. From the p_T distributions, we can find the yield of $X(3872)$ increases with increasing p_T in small p_T range, and decreases with increasing p_T in larger p_T range. However, the molecular state $X_M(3872)$ exhibits a narrower p_T distribution than the tetraquark state $X_T(3872)$ and nuclear-like state $X_N(3872)$ in the 0 – 10% centrality range. In the 30 – 50% centrality range, the p_T differential yields of the compact and nuclear-like state of the $X(3872)$ are smaller than that of the molecular state of the $X(3872)$, and their uncertainties are larger. The features of p_T distributions may be used to distinguish $X(3872)$ of different structure.

In Figure 3, we show the predicted pT-differential yields of the tetraquark, nuclear-like and molecular states of the $X(3872)$. We also analyze the pT-differential yield ratios for the $X(3872)$ and D^0, with the result shown in Figure 4.

From Figure 4, we observe that the yield ratio for the $X(3872)$ and D^0 in the centrality ranges of 0 – 10% is larger than that in the centrality ranges of 30 – 50%. In 0 – 10% centrality, the yield ratio for the molecular state of the $X(3872)$ and D^0 is lower than that for the tetraquark and nuclear-like states of the $X(3872)$. However, in 30 – 50% centrality, the yield ratio for the molecular state of the $X(3872)$ and D^0 is higher than that for the tetraquark and nuclear-like states of the $X(3872)$.

4 Conclusion

In this paper, we study the production of the $X(3872)$ in Pb-Pb collision at $\sqrt{s_{NN}} = 5.02$ TeV within the centrality ranges of 0 – 10% and 30 – 50% using the PACIAE + DCPC model. First, we investigate the dependence of the $X(3872)$ production on the mass uncertainty Δm and radius R. The results indicate that the yields of $X(3872)$ increase with the increasing Δm and R. We also predict the yield of the tetraquark, nuclear-like and molecular states of the $X(3872)$ in Pb-Pb collision at $\sqrt{s_{NN}} = 5.02$TeV for centralities of 0 – 10% and 30 – 50%, respectively. Subsequently, we examine the

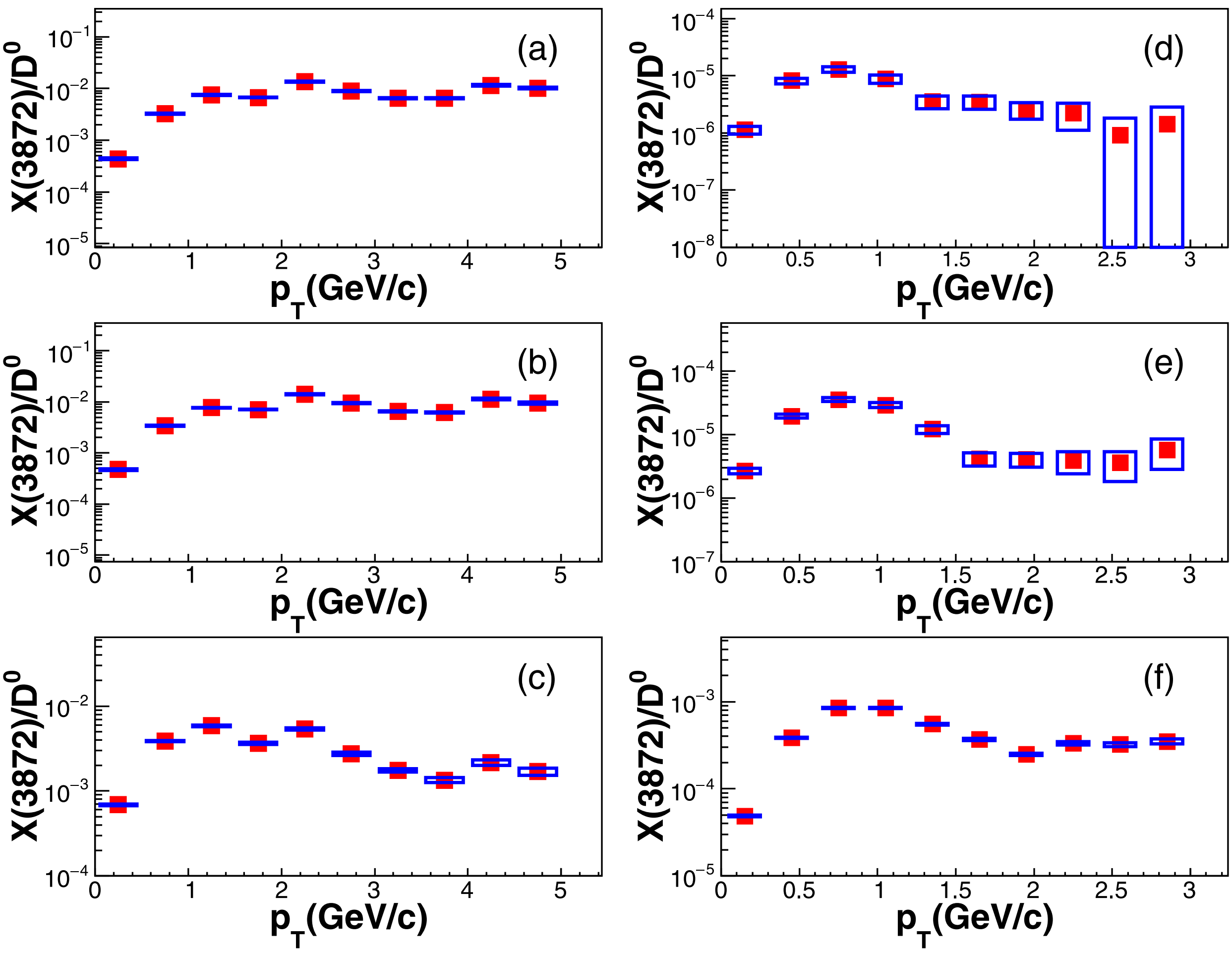

FIGURE 4
The yield ratio for $X(3872)$ and D^0 as a function of p_T in centralities of 0 – 10% (left panel) and 30 – 50% (right panel) in *Pb* – *Pb* collisions. The distribution in top, middle and bottom is the ratio for tetraquark, nuclear-like, molecular state of $X(3872)$ and D^0, respectively. The blue empty markers indicates statistical uncertainties, red filled markers indicates data point by PACIAE + DCPC model.

transverse momentum of these three different states of the $X(3872)$. We find that the p_T distributions of the $X(3872)$ for the three different structures are generally similar to each other. However, in the 0 – 10% centrality range, the molecular state $X_M(3872)$ exhibits a narrower p_T distribution than tetraquark state $X_T(3872)$ and nuclear-like state $X_N(3872)$.

Data availability statement

The original contributions presented in the study are included in the article/supplementary material, further inquiries can be directed to the corresponding author.

Author contributions

HX: Conceptualization, Data curation, Formal Analysis, Investigation, Methodology, Software, Validation, Writing – original draft, Writing – review and editing. ZS: Data curation, Resources, Software, Writing – review and editing. NY: Conceptualization, Funding acquisition, Project administration, Writing – review and editing. ZZ: Investigation, Methodology, Validation, Writing – review and editing.

Funding

The author(s) declare that financial support was received for the research and/or publication of this article. This work is supported by the Scientific Research Foundation of Hubei University of Education for Talent Introduction (No. ESRC20230002 and No. ESRC20230007) and Research Project of Hubei Provincial Department of Education (No. D20233003 and No. B2023191).

Conflict of interest

The authors declare that the research was conducted in the absence of any commercial or financial relationships that could be construed as a potential conflict of interest.

Generative AI statement

The author(s) declare that no Generative AI was used in the creation of this manuscript.

Publisher's note

All claims expressed in this article are solely those of the authors and do not necessarily represent those of their affiliated organizations, or those of the publisher, the editors and the reviewers. Any product that may be evaluated in this article, or claim that may be made by its manufacturer, is not guaranteed or endorsed by the publisher.

References

1. Gell-Mann M. A schematic model of baryons and mesons. *Phys. Lett.* (1964) 8:214–5. doi:10.1016/s0031-9163(64)92001-3

2. Zweig G, An SU_3 model for strong interaction symmetry and its breaking. Version 1 10.17181/CERN-TH-401 (1964).

3. Choi SK, Olsen SL, Abe T, Abe I, Adachi I, Aihara K, et al. Observation of a narrow charmonium-like state in exclusive $B^{\pm} \to K^{\pm}\pi^{+}\pi^{-}J/\psi$ decays. *Phys. Rev. Lett.* (2003) 91:262001. doi:10.1103/PhysRevLett.91.262001

4. Aubert B, Barate R, Boutigny D, Couderc F, Gaillard JM, Hicheur A, et al. Study of the $B \to J/\psi K^{-}\pi^{+}\pi^{-}$ decay and measurement of the $B \to X(3872)K^{-}$ branching fraction. *Phys. Rev. D* (2005) 71:071103. doi:10.1103/PhysRevD.71.071103

5. Acosta D, Affolder T, Ahn MH, Akimoto T, Albrow MG, Ambrose D, et al. (CDF), Observation of the narrow state $X(3872) \to J/\psi\pi^{+}\pi^{-}$ in $\bar{p}p$ collisions at $\sqrt{s} = 1.96$ TeV. *Phys. Rev. Lett.* (2004) 93:072001. doi:10.1103/PhysRevLett.93.072001

6. Abazov VM, Abbott B, Abolins M, Acharya BS, Adams DL, Adams M, et al. Observation and Properties of the X(3872) Decaying to $J/\psi\pi^{+}\pi^{-}$ in $p\bar{p}$ Collisions at $\sqrt{s} = 1.96$TeV. *Phys. Rev. Lett.* (2004) 93:162002. doi:10.1103/PhysRevLett.93.162002

7. Navas S, Amsler C, Gutsche T, Hanhart C, Hernández-Rey JJ, Lourenço C, et al. Review of particle physics*. *Phys. Rev. D* (2024) 110:030001. doi:10.1103/PhysRevD.110.030001

8. Liu MZ, Pan YW, Liu ZW, Wu TW, Lu JX, Geng LS. Three ways to decipher the nature of exotic hadrons: multiplets, three-body hadronic molecules, and correlation functions. *Phys. Rept.* (2025) 1108:1–108. doi:10.1016/j.physrep.2024.12.001

9. Chen H-X, Chen W, Liu X, Liu Y-R, Zhu S-L. An updated review of the new hadron states. *Rept. Prog. Phys.* (2023) 86:026201. doi:10.1088/1361-6633/aca3b6

10. Cho S, Furumoto T, Hyodo T, Jido D, Ko CM, Lee SH, et al. Identifying multiquark hadrons from heavy ion collisions. *Phys. Rev. Lett.* (2011) 106:212001. doi:10.1103/physrevlett.106.212001

11. Cho S, Hyodo T, Jido D, Ko CM, Lee SH, Maeda S, et al. Exotic hadrons from heavy ion collisions. *Prog. Part. Nucl. Phys.* (2017) 95:279–322. doi:10.1016/j.ppnp.2017.02.002

12. Hu Y, Liao J, Wang E, Wang Q, Xing H, Zhang H. Production of doubly charmed exotic hadrons in heavy ion collisions. *Phys. Rev. D* (2021) 104:L111502. doi:10.1103/physrevd.104.l111502

13. Chen CH, Xie YL, Xu HG, Zhang Z, Zhou DM, She ZL, et al. Exotic states $P_c(4312)$, $P_c(4440)$, and $P_c(4457)$ in pp collisions at $\sqrt{s} = 7$, 13 TeV. *Phys. Rev. D* (2022) 105:054013. doi:10.1103/PhysRevD.105.054013

14. Esposito A, Ferreiro EG, Pilloni A, Polosa AD, Salgado CA. The nature of X(3872) from high-multiplicity pp collisions. *Eur. Phys. J. C* (2021) 81:669. doi:10.1140/epjc/s10052-021-09425-w

15. Chen BY, Jiang L, Liu XH, Liu YP, Zhao JX. X(3872) production in relativistic heavy-ion collisions. *Phys. Rev. C* (2022) 105:054901. doi:10.1103/physrevc.105.054901

16. Sirunyan AM, Tumasyan A, Adam W, Ambrogi F, Bergauer T, Dragicevic M, et al. Evidence for X(3872) in Pb-Pb collisions and studies of its prompt production at $\sqrt{s_{NN}}$=5.02 TeV. *Phys. Rev. Lett.* (2022) 128:032001. doi:10.1103/PhysRevLett.128.032001

17. Xu HG, She ZL, Zhou DM, Zheng L, Kang XL, Chen G, et al. Investigation of exotic state X(3872) in pp collisions at $\sqrt{s} = 7$, 13 TeV. *Eur. Phys. J. C* (2021) 81:784. doi:10.1140/epjc/s10052-021-09573-z

18. Zhang H, Liao JF, Wang EK, Wang Q, Xing HX. Deciphering the nature of X(3872) in heavy ion collisions. *Phys. Rev. Lett.* (2021) 126:012301. doi:10.1103/physrevlett.126.012301

19. Grinstein B, Maiani L, Polosa AD. Radiative decays of $X(3872)$ discriminate between the molecular and compact interpretations. *Phys. Rev. D* (2024) 109:074009. doi:10.1103/physrevd.109.074009

20. Sa BH, Zhou DM, Yan YL, Li XM, Feng SQ, Dong BG, et al. PACIAE 2.0: an Updated parton and hadron cascade model (program) for the relativistic nuclear collisions. *Comput. Phys. Commun.* (2012) 183:333–46. doi:10.1016/j.cpc.2011.08.021

21. Sa BH, Zhou DM, Yan YL, Dong BG, Cai X. PACIAE 2.1: an updated issue of the parton and hadron cascade model PACIAE 2.0. *Comput. Phys. Commun.* (2013) 184:1476–9. doi:10.1016/j.cpc.2012.12.026

22. Zhou DM, Yan YL, Li XL, Li XM, Dong BG, Cai X, et al. An upgraded issue of the parton and hadron cascade model, PACIAE 2.2. *Comput. Phys. Commun.* (2015) 193:89–94. doi:10.1016/j.cpc.2015.01.022

23. Sjöstrand T, Mrenna S, Skands P. Pythia 6.4 physics and manual. *J High Energ Phys* (2006) 2006:026. doi:10.1088/1126-6708/2006/05/026

24. Chen G, Yan YL, Li DS, Zhou DM, Wang MJ, Dong BG, et al. Antimatter production in central Au+Au collisions at $\sqrt{s_{NN}}$=200 GeV. *Phys. Rev. C* (2012) 86:054910. doi:10.1103/physrevc.86.054910

25. Yan YL, Dong BG, Zhou DM, Li XM, Sa BH. Theoretical analysis for the apparent discrepancy between $\bar{p}p$ and pp data in charged particle forward-backward multiplicity correlations. *Phys. Lett. B* (2008) 660:478–82. doi:10.1016/j.physletb.2008.01.048

26. Zhou DM, Zheng L, Yan YL, Song ZH, Chen G, Li XM, et al. Impact of single string structure and multiple string interaction on strangeness production in Pb + Pb collisions at $\sqrt{s_{NN}} = 2.76$ TeV. *Phys. Rev. C* (2020) 102:044903. doi:10.1103/physrevc.102.044903

27. Zheng L, Zhou DM, Yin ZB, Yan YL, Chen G, Cai X, et al. Effect of single string structure and multiple string interaction on strange particle production in pp collisions at $\sqrt{s} = 7$ TeV. *Phys Rev C* (2018) 98:034917. doi:10.1103/physrevc.98.034917

28. Combridge BL, Kripfganz J, Ranft J. Hadron production at large transverse momentum and QCD. *Phys Lett B* (1977) 70:234–8. doi:10.1016/0370-2693(77)90528-7

29. Yan YL, Chen G, Li XM, Zhou DM, Wang MJ, Hu SY, et al. Predictions for the production of light nuclei in pp collisions at $\sqrt{s} = 7$ and 14 TeV. *Phys Rev C* (2012) 85:024907. doi:10.1103/physrevc.85.024907

30. Stowe K. *An introduction to thermodynamics and statistical mechanics*. 2nd ed. Cambridge University Press (2007).

31. Kubo R, Ichimura H, Usui T, Hashizume N. *Statistical mechanics: an advanced course with problems and solutions.* North-Holland Pub. Co (1965).

32. Ragab NA, She ZL, Chen G. The production of light (anti-)nuclei and (anti-)hypertriton in pp collisions at $\sqrt{s} = 0.9$, 2.76, and 7 TeV. *Eur Phys J Plus* (2020) 135:736. doi:10.1140/epjp/s13360-020-00735-8

33. Xu HG, Chen G, Yan YL, Zhou DM, Zheng L, Xie YL, et al. Study on the Ω_c^0 States Decaying to $\Xi_c^{+}K^{-}$ in pp collisions at $\sqrt{s} = 7$, 13 TeV. *Phys Rev C* (2020) 102:054319. doi:10.1103/PhysRevC.102.054319

34. Wu CT, She ZL, Peng XY, Kang XL, Xu HG, Zhou DM, et al. Study on the structure of exotic states $\chi c1(3872)$ via beauty-hadron decays in pp collisions at $\sqrt{s} = 8$ TeV. *Phys Rev D* (2023) 107:114022. doi:10.1103/physrevd.107.114022

35. Zhang Z, Zheng L, Chen G, Xu HG, Zhou DM, Yan YL, et al. The study of exotic state $Z_c^{\pm}(3900)$ decaying to $J/\psi\pi^{\pm}$ in the pp collisions at $\sqrt{s} = 1.96$, 7, and 13 TeV. *Eur Phys J C* (2021) 81:198. doi:10.1140/epjc/s10052-021-08983-3

36. Liu FX, Chen G, She ZL, Zheng L, Xie YL, Dong ZJ, et al. ${}^{3}_{\Lambda}H\ and\ {}^{3}_{\bar{\Lambda}}\overline{H}$ production and characterization in Cu+Cu collisions at $\sqrt{s_{NN}} = 200$GeV. *Phys Rev C* (2019) 99:034904. doi:10.1103/PhysRevC.99.034904

37. Liu FX, Chen G, Zhe ZL, Zhou DM, Xie YL. Light (anti)nuclei production in Cu+Cu collisions at $\sqrt{s_{NN}} = 200$ GeV. *Eur Phys J A* (2019) 55:160. doi:10.1140/epja/i2019-12851-x

38. Chen G, Chen H, Wu J, Li DS, Wang MJ. Centrality dependence of light (anti)nuclei and (anti)hypertriton production in Au+Au collisions at $\sqrt{s_{NN}}$=200 GeV. *Phys Rev C* (2013) 88:034908. doi:10.1103/physrevc.88.034908

39. Chen G, Chen H, Wang JL, Chen ZY. Scaling Properties of light (anti)nuclei and (anti)hypertriton production in Au+Au collisions at $\sqrt{s_{\mathrm{NN}}} = 200$ GeV. *J Phys G* (2014) 41:115102. doi:10.1088/0954-3899/41/11/115102

40. Dong ZJ, Chen G, Wang QY, She ZL, Yan YL, Liu FX, et al. Energy dependence of light (anti)nuclei and (anti)hypertriton production in the Au-Au collision from $\sqrt{s_{NN}} =$ 11.5 to 5020 GeV. *Eur Phys J A* (2018) 54:144. doi:10.1140/epja/i2018-12580-8

41. She ZL, Chen G, Liu FX, Zheng L, Xie YL. Study of nuclear modification factors of (anti-)hadrons and light (anti-)nuclei in Pb-Pb collisions at $\sqrt{s_{\mathrm{NN}}} = 2.76$ TeV (2019).

42. She ZL, Gang C, Xu HG, Zeng TT, Li DK. Centrality dependence of light (anti)nuclei and (anti)hypertriton production in Pb-Pb collisions at $\sqrt{s_{NN}} = 2.76$ TeV. *Eur Phys J A* (2016) 52:93. doi:10.1140/epja/i2016-16093-2

43. Acharya S, Adamová D, Adhya SP, Adler A, Adolfsson J, Aggarwal MM, et al. Production of charged pions, kaons, and (anti-)protons in Pb-Pb and inelastic *pp* collisions at $\sqrt{s_{NN}} = 5.02$ TeV. *Phys Rev C* (2020) 101:044907. doi:10.1103/PhysRevC.101.044907

44. Acharya S, Adamová D, Adler A, Adolfsson J, Agnello M, Agrawal N, et al. Prompt D^0, D^+, and D^{*+} production in Pb–Pb collisions at $\sqrt{s_{\mathrm{NN}}} = 5.02$ TeV. *J High Energ Phys* (2022) 174. doi:10.1007/JHEP01(2022)174

45. Yan YL, Zhou DM, Lei AK, Li XM, Zhang XM, Zheng L, et al. Revisiting the centrality definition and observable centrality dependence of relativistic heavy-ion collisions in paciae model. *Comput Phys Commun* (2023) 284:108615. doi:10.1016/j.cpc.2022.108615